Scripta Materialia 159 (2019) 99–103

Contents lists available at ScienceDirect

Scripta Materialia

journal homepage: www.elsevier.com/locate/scriptamat

Interfacial stability of θ'/Al in Al-Cu alloys

Kyoungdoc Kim, Bi-Cheng Zhou, C. Wolverton *

Department of Materials Science and Engineering, Northwestern University, Evanston, IL 60208, United States

ARTICLE INFO

Article history:
Received 3 June 2018
Received in revised form 2 August 2018
Accepted 12 September 2018
Available online xxxx

Keywords:
First-principles calculation
Aluminum alloys
Al-Cu
θ' precipitate
Interfacial energy

ABSTRACT

Designing low-energy interface structures is crucial in growth and coarsening studies of Al_2Cu (θ') precipitates. Given new experimental insights into the θ'/Al system, we use Density Functional Theory (DFT) calculations to investigate the energetics of the coherent $(001)_{\theta'}//(001)_{Al}$ and semi-coherent $(010)_{\theta'}//(010)_{Al}$ interfaces. We find that the recently proposed occupancy of interstitial Cu atoms at the coherent interface by Bourgeois et al. increases interfacial energy, and hence, is likely due to kinetic effects. For the semi-coherent interface, the semi-coherent interfacial energy does not significantly depend on interfacial configurations or misfit strains up to 10-unit cells of Al.

Precipitation hardening represents a significant source of strength in aluminum alloys and Al_2Cu (θ') is one of the most common and effective strengthening precipitate phases [1–3]. In Al-Cu alloys, a series of metastable precipitate phases are formed from the decomposition of a supersaturated solid solution during precipitation [4,5]. At relatively low aging temperatures, the sequence of steps for the Al-Cu precipitation process is: Al_{ss} → Guinier Preston (GP I zones) → θ'' (GP II zones) → θ' → θ [6,7]. The crystal structure of the θ' phase is a CaF_2 structure, but, when embedded in an Al matrix, it adopts a tetragonally distorted version of a cubic fluorite (C1) structure with lattice constants of a = 4.04 Å and c = 5.80 Å. The morphology of the θ' precipitate is a plate-like morphology with an extremely high aspect ratio (θ' plates are typically 1–10 nm in thickness and 0.1–1 μm in length [8]), and this high aspect ratio serves an important role as an effective strengthening component. There are two different crystallographic interfacial orientations of the plate-shaped precipitate phase. One is a coherent interface $(001)_{\theta'}//(001)_{Al}$ on the broad faces of the plate, and the other is a semi-coherent interface with $(010)_{\theta'}//(010)_{Al}$ around the rim of the plates [9]. The interfacial energy plays a significant role in determining the precipitate morphology, since it in part determines the height of the energy barrier for nucleation and the number density of nuclei, thereby influencing the size distribution of the precipitate. Also, knowledge of interfacial energies coupled with misfit strains can be used to determine the growth and equilibrium morphology of precipitates [10–12]. Thus, a detailed understanding of the thermodynamically stable interfacial structure and its energy is a key step for understanding various precipitate-related phenomena.

The crystal structure and the interfacial energy of the $\theta'//\alpha$-Al interfaces have been studied both experimentally [8,9,13] and computationally [11,12,14]. All the previous models of the interfacial structure are based on a simple termination of the bulk crystal structures of fluorite Al_2Cu and fcc Al. However, Bourgeois et al. [15] recently called these models into question because they found a new structure for the coherent interface, distinct from the previously accepted structures based on a simple termination of the $(001)_{\theta'}$ facet of the precipitate. They referred to their finding as an intermediate phase in the growth of the θ' precipitate, and referred to the structure as a "GP (I) zone-like interface". The newly proposed interface has a different composition and crystal structure, with extra interstitial Cu atoms relative to the bulk-terminated interface $\theta'//\alpha$-Al. Bourgeois et al. argue that during the evolution of the precipitates, the Cu atoms move from these interstitial positions to create new lattice sites of θ', thereby causing growth of the θ' precipitate. Thus, these interstitial Cu atoms are responsible for precipitate ledge growth. In order to clearly understand the energetic behavior of this interstitial Cu occupancy on the interfacial stability, we perform interfacial energy calculations for both the previously proposed structure as well as this newly-proposed one.

The semi-coherent interfacial energy (around the rim of θ' precipitates) is an important component to the nucleation energy barrier, and information regarding interfacial energy coupled with misfit strains is also important to understanding precipitate growth. For example, the calculated interfacial energies and lattice misfit strains can be incorporated into a meso-scale phase field model to understand the equilibrium θ' morphology [10–12]. Thus, we investigate the semi-coherent interfacial energy of interfaces with different configurations (combinations of different number of unit-cells of α-Al and θ') by using first-principles DFT calculations.

* Corresponding author.
E-mail address: c-wolverton@northwestern.edu (C. Wolverton).

https://doi.org/10.1016/j.scriptamat.2018.09.018
1359-6462/

Here, we perform atomic-scale density functional theory (DFT) calculations to explore the thermodynamically stable interfacial structure and energies at the coherent and semi-coherent θ'//α-Al interfaces. Our analysis of the energies and structures of θ' interfaces will be helpful for future studies of the nucleation and evolution of these precipitates.

We performed first-principles DFT calculations using the Vienna Ab initio Simulation Package (VASP) [16,17] and projector-augmented wave potentials [18]. We utilized the PBE parameterization of the generalized gradient approximation (GGA-PBE) [19] for all calculations. All structures were relaxed with respect to all cell-internal and cell-external degrees of freedom at an energy cutoff of 450 eV. In the calculation of formation energy, gamma-centered k-point meshes were constructed to achieve at least 9000 k-points per reciprocal atom, and the convergence of the energy differences was within 1 meV/atom. For interfacial energy calculations, k-point meshes were used to achieve approximately 10,000 k-points per reciprocal atom. And different super cell sizes were tested for convergence of the interfacial energies, finding differences on the order of 5–10%. In the calculation of solute segregation, $2 \times 2 \times 1$ super cells (180 and 188 atoms) were used to achieve the segregation energy of each bulk phase, and a $7 \times 7 \times 1$ k-point mesh was used to achieve 9000 k-points per reciprocal atom for converged energy differences within 0.03 eV/solute atom. A k-point mesh of "1" for the direction of out of the interface was enough for convergence within 0.02 eV/solute atom. For segregation of solute near the interface with interstitial Cu atoms, an $8 \times 8 \times 1$ k-point mesh was used with convergence within 0.01 eV/solute atom.

We construct supercells of θ' and α-Al to calculate the interfacial energies of the θ'//α-Al interfaces. The energy of formation per atom relative to the energies of α-Al and θ' phases can be written as follows [12]:

$$\Delta E_f = \delta E_{cs\ (\alpha,\theta')} + \frac{2\sigma A}{N} \tag{1}$$

where $\delta E_{cs\ (\alpha,\theta')}$ is the coherency strain per atom caused by the lattice mismatch between α-Al and θ'. N is the total number of atoms in the super cell, and σ and A are the interfacial energy and area, respectively. ΔE_f is computed as follows

$$\Delta E_f = \left[E_{Al_{a+2b}Cu_b(\alpha,\theta')} - E_{Al_a(\alpha)} - E_{Al_{2b}Cu_b(\theta')}\right]/N \tag{2}$$

where $E_{Al_{a+2b}Cu_b(\alpha,\theta')}$ is a total energy of supercells in DFT calculations, and $E_{Al_a(\alpha)}$ and $E_{Al_{2b}Cu_b(\theta')}$ are calculated DFT bulk energies of θ' and α-Al, respectively. Based on Eq. (1), we can obtain the interfacial energy from the slope of ΔE_f vs. $1/N$ as shown in Fig. 1(b). The detailed explanation about the interfacial energy calculation method is described in [12]. In Eq. (2), the number of Cu atoms in a supercell is balanced by number of Cu atoms in θ', and the remaining number of Al atoms in a supercell is balanced by pure Al. Basically, this is an analogous approach to using chemical potentials from the stable phases on the convex hull which we recently used in [20]. For the calculation of Si segregation energies (ΔE_{seg}), we use the same method as shown in [21] with two reference phases, α-Al and θ'.

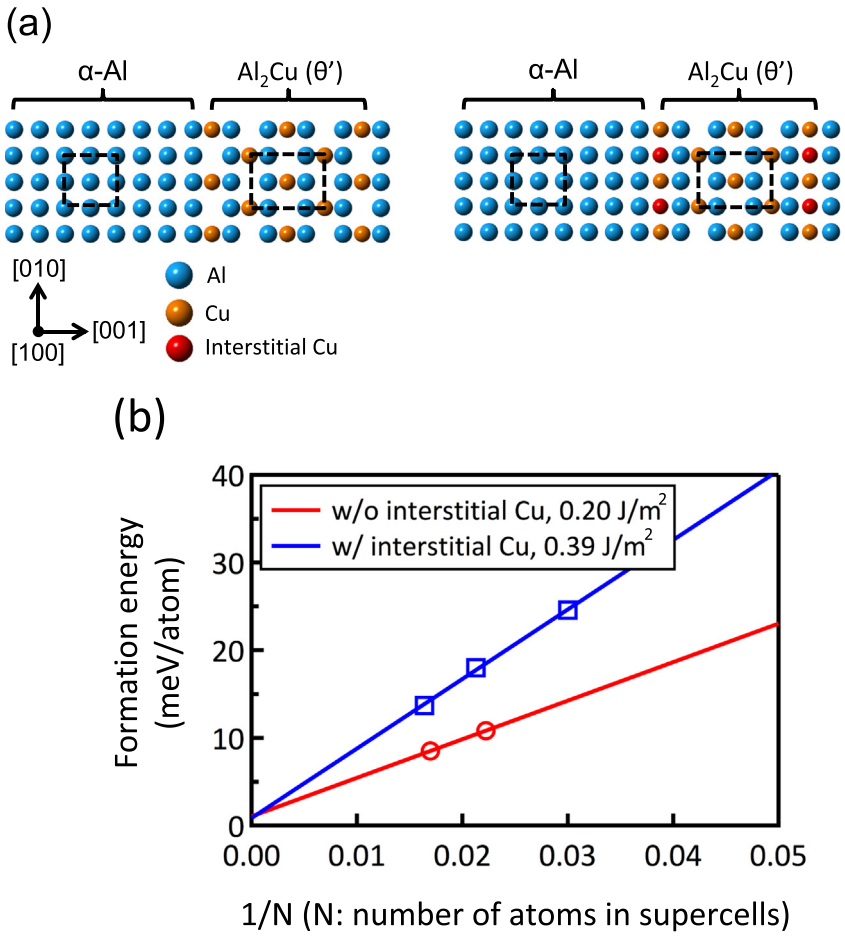

Fig. 1. (a) Relaxed atomic models and schematic diagrams for the coherent $(001)_{\theta'}/(001)_{Al}$ interface used in our first-principles calculations. (Left) without occupancy of interstitial Cu atoms (Right) with occupancy of interstitial Cu atoms at the interface. The blue spheres represent Al atoms, the orange spheres represent Cu atoms, and the red spheres represent interstitial Cu atoms at the interface, respectively. (b) First-principles formation energies of the coherent N-atom super cells as a function of $1/N$ for the interface without or with interstitial Cu atoms, as shown in (a, left) and (a, right). The energies of the large-cell calculations were fitted to straight lines, and the interfacial energies (σ) were extracted from the slopes, 2σA, of these lines by Eq. (1). (For interpretation of the references to color in this figure legend, the reader is referred to the web version of this article.)

Since the two-phase equilibrium in binary Al-Cu is between α-Al and θ', Al_2Cu (θ') is the lowest energy state ("per Cu") in equilibrium with α-Al at 0 K. In other words, the Cu chemical potential is lowest for α-Al and θ' at 0 K. Thus, we choose α-Al and θ' for the reference phases for the energetic comparison between the two coherent interfaces with and without interstitial Cu atoms in this work. The tetragonal structure (C16) of Al_2Cu (θ) is not stable in $T = 0$ K DFT calculations. This was explained by the role of the vibrational entropies of θ and θ', which were found to be unexpectedly important for this phase [22]. We use pure Al as a reference state rather than the Al-Cu solid solution because the solubility of Cu in Al is small (0.001 X_{Cu}) even at typical θ' aging temperatures (250 °C) based on recent thermodynamic (CALPHAD) modeling of the Al-Cu system [23–25].

To clarify the energetic effect of the Cu interstitial occupancy on interfacial thermodynamic stability, we first perform interfacial energy calculation for interfaces with and without interstitial Cu. Fig. 1(a) shows the interface supercell between Al_2Cu (θ') and the Al matrix. For interfacial energy calculations, the energies of two separate phases are computed in Eq. (2). However, it is impossible to calculate isolated bulk θ' structure with the extra Cu atoms due to periodic boundary conditions. More importantly, since the two-phase equilibrium in binary Al-Cu is between α-Al and θ', the physical situation dictates the choice of α-Al and θ' for the reference phases for the energetic comparison between the two coherent interfaces with and without interstitial Cu atoms. Therefore, we use energies of the equilibrium phases α-Al and pure θ' for ΔE_f in Eq. (2). In Eq. (2), the number of Cu atoms in the supercell is balanced by number of Cu atoms in θ', and the remaining number of Al atoms is balanced by pure Al phase. Fig. 1(b) shows that the coherent interface (Left image in Fig. 1(a)) has an interfacial energy of 0.20 J/m^2. However, a much larger interfacial energy of 0.39 J/m^2 was obtained for the interface with occupancy of interstitial Cu atoms (Right image in Fig. 1 (a)), indicating that the interstitial occupancy is not energetically preferred according to our computations. In other words, we find that interstitial Cu atoms decrease interfacial stability compared to an interface without interstitial Cu atoms based on two stable phases in binary Al-Cu, α-Al and θ'.

Commercial cast aluminum alloys are complex multi-component systems, and Si is a common element in many commercial alloys. The study of interfacial segregation of solute atoms is important because the interfacial energy of the matrix-precipitate interface is strongly influenced by the chemistry of the interface, thereby influencing the morphology of precipitates. For example, according to the literature [21], Si has a role in catalyzing the heterogeneous nucleation of GPII zones and θ' precipitates by interfacial segregation in the Al-Cu system. Here, to investigate the effect of interstitial occupancy by Cu atoms on the segregation of Si solute in a ternary alloying system, we compared the segregation energies of the Si solute both interfaces to previous APT results by Biswas et al. [21,26] in Fig. 2(a)–(c). The previous APT results [21,26] showed that Si atoms strongly segregate at the coherent interface. Specifically, previous first-principles calculations (validated by red points finding favorable segregation energies for Si in our work, as shown in Fig. 2(c)) aptly explained the experimental segregation behavior based on non-interacting solute atoms at the coherent interface without interstitial Cu atoms. We have extended these calculations to segregation in the presence of interstitial Cu atoms. In Fig. 2(c), we see that the Si segregation changes qualitatively in the presence of

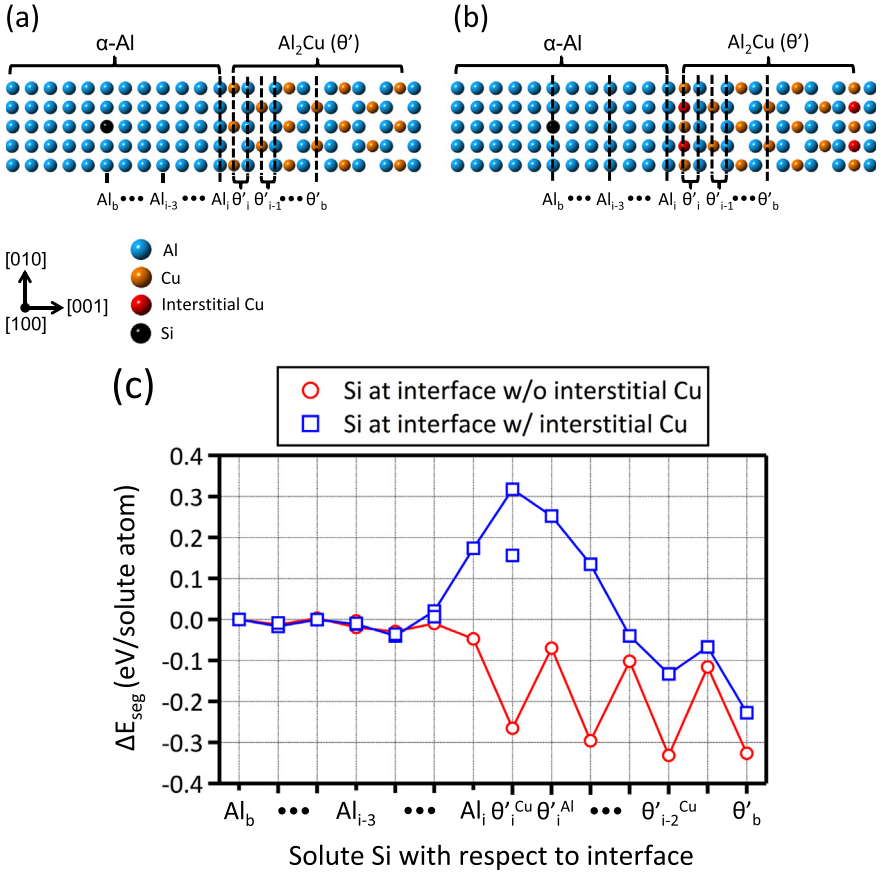

Fig. 2. (a) and (b) Relaxed atomic models for the coherent $(001)_{\theta'}/(001)_{Al}$ interface: The blue spheres represent Al atoms, the orange spheres represent Cu atoms, and the red spheres represent interstitial Cu atoms (on θ_f-plane), respectively. The black atom in the supercell illustrates the position of a Si atom at a bulk-like site in the Al matrix. (Sub) lattice planes are labeled according to their position relative to the interface planes. For example, Al_i refers the Al plane adjacent to the interface; Al_b refers to a bulk-like plane in the Al matrix; and θ_i^{Cu} refers to the interfacial Cu layer within the θ' precipitate. (c) Calculated Si solute segregation energies as a function of distance from the coherent interfaces. Two segregation energies are reported for each layer. The blue points represent Si solute at the coherent interface with the interstitial Cu atoms at interface, and the red points represent Si solute at the coherent interface without interstitial Cu atoms at interface. The sites that have a sign convention of $\Delta E_{seg}<0$ are energetically favorable compared to Al bulk-like sites in the matrix. (For interpretation of the references to color in this figure legend, the reader is referred to the web version of this article.)

interstitial Cu: Si does not preferentially segregate to the interface with interstitial Cu atoms (ΔE_{seg} >0.1 eV/atom solute on Al_i~$\theta_{i-i}Cu$ planes), which is in disagreement with APT results [21,26]. Thus, the segregation behavior also points to the conclusion that the interstitial Cu are not a stable part of the equilibrium interface, but rather are a kinetically controlled state formed during growth of θ'.

Semi-coherent interfacial structure and the corresponding energy around the rim of θ' precipitate is important because it is responsible for factors, such as the shape, solute segregation, and growth or coarsening rates of precipitates [27]. One interesting aspect is that the residual misfit strains at a semi-coherent interface vary with different interfacial configurations during the thickening process [9,28]. Moreover, lengthening kinetics is affected by a thickness-dependent misfit strain based on the previous literature [29]. Thus, the information about semi-coherent interfacial energy coupled with thickness-dependent misfit strains is crucial for the study of θ' morphology [10].

Recent observations of the distribution of θ' thicknesses show a variation with $0.5C_{\theta'}$ steps [30]. The most commonly observed thicknesses are $2C_{\theta'}$ and $3.5C_{\theta'}$ for 200 °C/24 h aging [30]. In the previous work by Hu et al. [14], the modified embedded-atom method (MEAM) potentials were used to calculate semi-coherent interfacial energies with different interfacial configurations, and the results showed that an interfacial configuration $2C_{\theta'}$:$3a_{Al}$ with misfit strain (−4.29% [14] or −5.1% [12]) is energetically favored. However, their study did not investigate the $7C_{\theta'}$:$10a_{Al}$ (=$3.5C_{\theta'}$:$5a_{Al}$) configuration, which is the lowest misfit strain (−0.3% [12] or +0.45% [31]) among all the possible combinations of number of unit-cells of α-Al and θ' up to 10-unit cells of Al. This configuration is important because when a semi-coherent interface has $7C_{\theta'}$:$10a_{Al}$ (=$3.5C_{\theta'}$:$5a_{Al}$) configuration, the effect of elastic energy anisotropy becomes smaller. This strongly influences equilibrium θ' morphology [10]. The lengthening kinetics are also strongly influenced by a thickness-dependent misfit strain [29]. Thus, we also use first-principles calculations to investigate the thermodynamic stability of a semi-coherent interface with different misfit configurations including a $7C_{\theta'}$:$10a_{Al}$ (=$3.5C_{\theta'}$:$5a_{Al}$) match.

Fig. 3(a) and (b) represent the relationship between interface configuration and its interfacial energy, i.e., how many θ' and α-Al unit cells match each other. We investigated semi-coherent interfacial configurations, $2C_{\theta'}$:$3a_{Al}$, $3C_{\theta'}$:$4a_{Al}$, $7C_{\theta'}$:$10a_{Al}$ (=$3.5C_{\theta'}$:$5a_{Al}$). Each interfacial configuration shows different lattice misfit strains −4.56%,

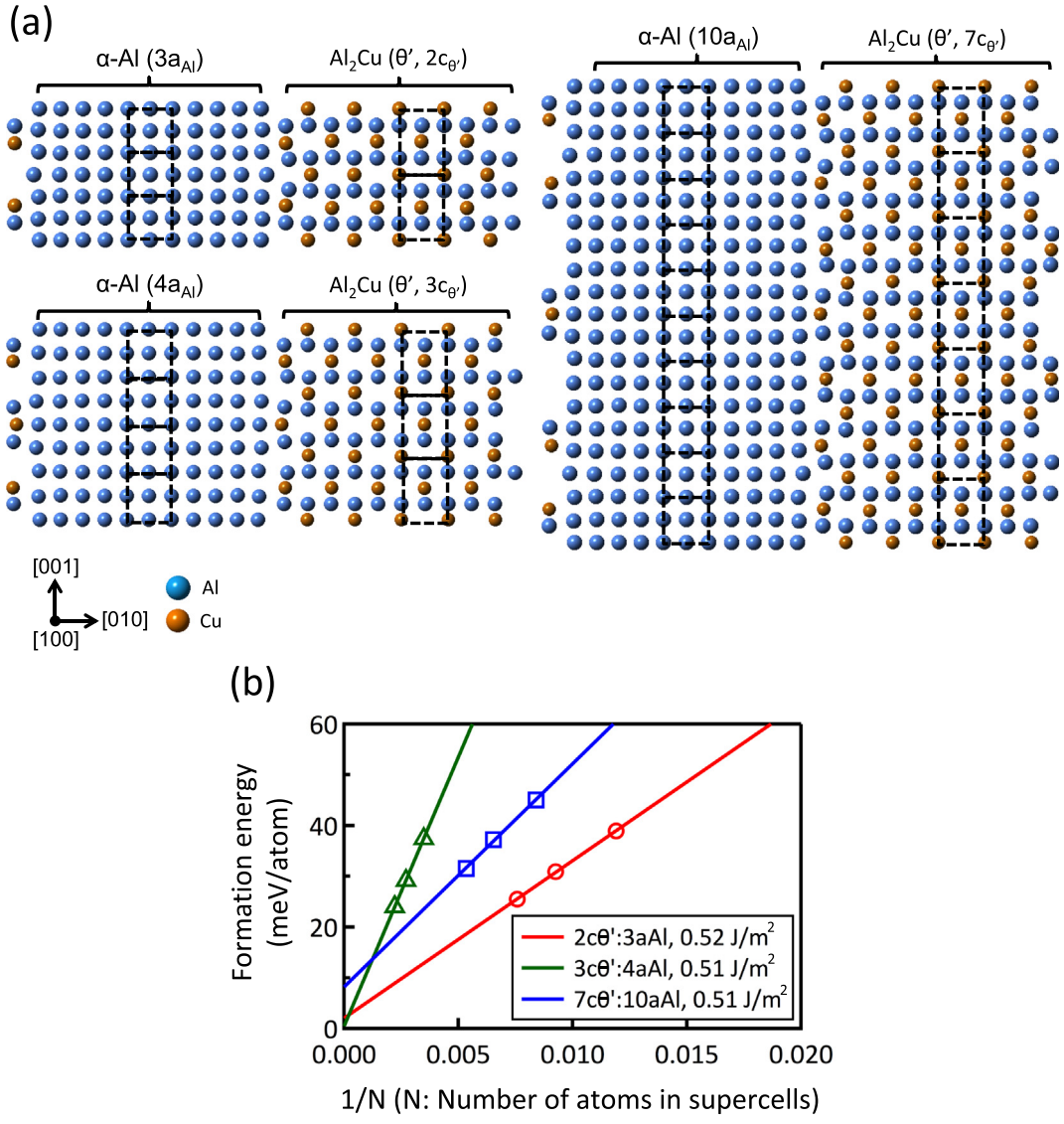

Fig. 3. (a) Relaxed atomic models for the semi-coherent $(010)_{\theta'}/(010)_{Al}$ interface with different interfacial configurations, $2C_{\theta'}$:$3a_{Al}$, $3C_{\theta'}$:$4a_{Al}$, $7C_{\theta'}$:$10a_{Al}$ (=$3.5C_{\theta'}$:$5a_{Al}$), which corresponds to lattice misfit strains, −4.56%, +7.37%, +0.22%, were used in our first-principles calculations (b) First-principles formation energies of $(010)_{\theta'}//(010)_{Al}$ N-atom supercells as a function of 1/N for the interface. The energies of the large-cell calculations were fitted to straight lines, and the interfacial energies (σ) were extracted from the slopes, $2\sigma A$, of these lines by Eq. (1). The interface with the $7C_{\theta'}$:$10a_{Al}$ (=$3.5C_{\theta'}$:$5a_{Al}$) configuration has a higher slope, but also a relatively higher interfacial area of larger supercells, and as such, extracted interfacial energies are similar.

+7.37%, +0.22%. They are similar to those reported in the literature, which are −4.29% [14] or −5.1% [12], +6.8% [12] or +7.67% [14], and −0.3% [12] or +0.45% [31], respectively. For the configuration of $7C_{\theta'}$:$10a_{Al}$ (=$3.5C_{\theta'}$:$5a_{Al}$), we chose very large supercells with a $7C_{\theta'}$:$10a_{Al}$ configuration instead of choosing $3.5C_{\theta'}$:$5a_{Al}$ because the a $7C_{\theta'}$:$10a_{Al}$ configuration satisfies the periodic boundary condition of Cu atoms along the [001] axis in Fig. 3(a). As shown in Fig. 3(b), the three calculated interfacial energies were remarkably similar (0.51, 0.51, and 0.52 J/m^2), which is largely consistent with the previous literature [14] using the MEAM potentials. In conclusion, we argue that misfit strain energy does not significantly influence the semi-coherent interfacial energy. That is, the semi-coherent interfacial energy is not significantly dependent upon the interface configurations.

This study focused on the thermodynamic stability of the coherent $(001)_{\theta'}//(001)_{Al}$ and semi-coherent $(010)_{\theta'}//(010)_{Al}$ interfaces. We found that the interstitial Cu occupancy increases the interfacial energy, which means that the interfacial stability of a coherent interface decreases. In ternary Al-Cu-Si, the interstitial Cu atoms change the segregation behavior of the Si atoms; a tendency that is inconsistent with the previous results obtained using atom probe tomography (APT), which showed that strong segregation exists at the interface. Therefore, we conclude that a coherent interface without interstitial Cu atoms corresponds to an equilibrium interfacial state. Future kinetic studies will be needed to fully explain the experimentally observed occupancy of interstitial Cu atoms at the coherent interface. Additionally, we investigated the energetically favored interfacial configuration at a semi-coherent interface, a match between different numbers of unit-cells of θ' and α-Al, for the future study of nucleation or growth of θ' precipitate. The results demonstrate that a semi-coherent interfacial energy does not significantly depend on the semi-coherent interfacial configurations or misfit strains up to 10-unit cells of Al.

Acknowledgements

K. K. acknowledges support from the US Department of Energy under award number DE-EE0006082. Portions of this work were supported by The Center for Hierarchical Materials Design (CHiMaD), Dept. of Commerce, NIST under award number 70NANB14H012. We gratefully acknowledge the computing resources from Quest high performance facility.

References

[1] A. Wilm, Metallurgie, Vol. 8, , 1911.
[2] L.F. Mondolfo, Aluminum Alloys: Structure and Properties, Butterworths, 1976.
[3] F.W. Gayle, M. Goodway, Science 266 (5187) (1994) 3.
[4] G.W. Lorimer, Precipitation Processes in Solids, Metallurgical Society of the AIME, Warrendale, 1978.
[5] D.A. Porter, K.E. Easterling, Phase Transformations in Metals and Alloys, 2nd edition Chapman & Hall, London, 1992.
[6] G.D. Preston, Nature 142 (1938).
[7] J.M. Silcok, T.J. Heal, H.K. Hardy, J. Inst. Met. 82 (1953–1954) 239–248.
[8] H.I. Aaronson, J.B. Clark, C. Laird, Met. Sci. J. 2 (1968).
[9] W.M. Stobbs, G.R. Purdy, Acta Metall. 26 (7) (1978) 13.
[10] K. Kim, A. Roy, M.P. Gururajan, C. Wolverton, P.W. Voorhees, Acta Mater. 140 (Supplement C) (2017) 344–354.
[11] V. Vaithyanathan, C. Wolverton, L.Q. Chen, Phys. Rev. Lett. 88 (12) (2002), 125503.
[12] V. Vaithyanathan, C. Wolverton, L.Q. Chen, Acta Mater. 52 (10) (2004) 2973–2987.
[13] G.C. Weatherly, Acta Metall. 19 (3) (1971) 181–192.
[14] S.Y. Hu, M.I. Baskes, M. Stan, L.Q. Chen, Acta Mater. 54 (18) (2006) 4699–4707.
[15] L. Bourgeois, C. Dwyer, M. Weyland, J.-F. Nie, B.C. Muddle, Acta Mater. 59 (18) (2011) 7043–7050.
[16] G. Kresse, J. Furthmüller, Phys. Rev. B 54 (16) (1996) 11169–11186.
[17] G. Kresse, J. Furthmüller, Comput. Mater. Sci. 6 (1) (1996) 15–50.
[18] G. Kresse, D. Joubert, Phys. Rev. B 59 (3) (1999) 1758–1775.
[19] J.P. Perdew, K. Burke, M. Ernzerhof, Phys. Rev. Lett. 77 (18) (1996) 3865–3868.
[20] K. Kim, A. Bobel, V. Brajuskovic, B.-C. Zhou, M. Walker, G.B. Olson, C. Wolverton, Acta Mater. 154 (2018) 207–219.
[21] A. Biswas, D.J. Siegel, C. Wolverton, D.N. Seidman, Acta Mater. 59 (15) (2011) 6187–6204.
[22] C. Wolverton, V. Ozoliņš, Phys. Rev. Lett. 86 (24) (2001) 5518–5521.
[23] C. Jiang, Z.-K. Liu, Acta Mater. 51 (15) (2003) 4447–4459.
[24] L. Kaufman, H. Bernstein, Computer Calculation of Phase Diagrams, Academic Press, New York, 1970.
[25] N. Saunders, in: I. Ansara, A.T. Dinsdale, M.H. Rand (Eds.), COST 507: Thermochemical Database for Light Metal Alloys, Vol. 2, European Commission, 1998.
[26] A. Biswas, D.J. Siegel, D.N. Seidman, Phys. Rev. Lett. 105 (7) (2010), 076102.
[27] L. Bourgeois, N.V. Medhekar, A.E. Smith, M. Weyland, J.-F. Nie, C. Dwyer, Phys. Rev. Lett. 111 (4) (2013), 046102.
[28] J.-F. Nie, in: D.E. Laughlin, K. Hono (Eds.), Physical Metallurgy, fifth editionElsevier, Oxford 2014, pp. 2009–2156.
[29] Y. Li, G. Purdy, Acta Mater. 56 (3) (2008) 364–368.
[30] L. Bourgeois, C. Dwyer, M. Weyland, J.-F. Nie, B.C. Muddle, Acta Mater. 60 (2) (2012) 633–644.
[31] G.R. Purdy, J.P. Hirth, Philos. Mag. Lett. 86 (3) (2006) 147–154.